Calibration sources of Čerenkov radiation

R. J. Boardman, M. D. Lay,
N. W. Tanner, D. L. Wark

Nuclear Physics Laboratory,
University of Oxford,
Keble Road, Oxford,
OX1 3RH.

April 23, 1991

To be submitted to
Nuclear Instruments and Methods.

Abstract

We report on attempts to construct and simulate low intensity sources of Čerenkov radiation with accurately known spectral intensity. These sources will be used to calibrate photomultipliers for the Sudbury Neutrino Observatory.

We have used ^{90}Sr as a radioactive beta source located at the center of a sphere of ultraviolet transparent acrylic. The production of Čerenkov radiation by stopping electrons in acrylic has been calculated (by several methods) using the theory of Frank and Tamm. The systematic effects of the variation of the refractive index with frequency have also been considered. The propagation of the Čerenkov radiation out of the sphere has been studied with reference to the problem of total internal reflection. The total Čerenkov radiation output of these spheres from a single decay is calculated with a systematic uncertainty of a few percent. The amount of activity in each source also contributes to the uncertainty of the Čerenkov radiation intensity at the one percent level.

1 Introduction

The Sudbury Neutrino Observatory (SNO) [1] is being constructed to resolve the solar neutrino problem. The SNO detector will measure the charged current and neutral current weak interactions of solar neutrinos in 1000 tonnes of D_2O contained in an acrylic vessel. A shield of H_2O, and the use of materials with low radioactive contamination, will reduce internal backgrounds. The location of the detector in the Creighton mine of INCO Limited, at a depth of 2070 m, will ensure that cosmic-ray backgrounds are reduced. Interactions in the D_2O produce relativistic electrons which emit Čerenkov radiation. This light is monitored by approximately 10^4 photomultiplier tubes mounted on a sphere of radius 8.5 m, which surrounds the D_2O, see figure 1. These photomultipliers have bi-alkali (K_2 Cs Sb) photocathodes of 20 cm diameter, and have a single photoelectron peak. The use of optical reflectors will double the amount of light detected, giving an effective coverage of about 60 %. Estimates of the detection efficiency suggest that only 10 Čerenkov photons are detected per MeV of electron energy. The number, time and position of these hits gives information about the energy, direction and location of the electron.

An accurate energy calibration of the detector is crucial to the determination of the detector energy threshold and the energy spectrum of the neutrinos. Energy calibration will be done using radio-active sources and regular optical sensitivity checks. Measurements of the absolute efficiency of photomultiplier tubes (preferably in the detector) will be a useful check of the energy calibration. Photocathode quantum efficiency can be estimated from the photoelectric current yield from illumination by a relatively bright source. However, the collection and multiplication of these photoelectrons is not perfect, and the single photoelectron counting efficiency is typically lower than the quantum efficiency by several tens of percent. Unfortunately, the absolute single photon efficiency requires a light source of very low intensity, and there are few accurately calibrated light sources with intensities in the required range, 10^{-8} to 10^{-6} Hz per unit angular frequency.

Black body sources have been used to provide calibrated low intensity light sources, but their intensity spectrum is not well matched to the response of a photomultiplier photocathode. Neutral density filter methods have also been used with some success [2, 3]. The intensity spectrum of these sources is adequate for the estimation of electron collection efficiency, but a Čerenkov source is more suitable for predicting the response of photomultipliers in the SNO detector. The early work of Belcher *et al* [4, 5], developed such calibrated sources using dilute solutions containing radioactive beta sources. Of the isotopes used ^{90}Sr has the longest life and the highest yield per unit activity of parent nucleus. Also, the decays of ^{90}Sr and its daughter ^{90}Y are essentially free of electromagnetic transitions, thus simplifying the predictions of Čerenkov radiation.

We have attempted to construct and simulate low intensity Čerenkov sources by depositing a known amount of ^{90}Sr inside an acrylic sphere with known properties. Such sources will be used to calibrate photomultipliers and could be used inside the SNO detector to provide calibration in situ. Some prototype sources have been used for single photon collection efficiency measurements. With the yields deduced in this paper, the first dynode collection efficiencies obtained were in the expected range, approximately 70 $\rightarrow$ 100 %, depending on the operating conditions. We have also used them to measure photomultiplier transit time spread, using methods similar to Present *et al* [7]. These sources are relatively compact and could have wider applications in calibration photometry.

2 Acrylic spheres

The ^{90}Sr was located in acrylic spheres of radius r which have hollow centers of radius r_i to accommodate the radioactive isotope. See figure 2. The inner and outer radii of the sources are constrained by the problem of total internal reflection, which can lead to the capture of Čerenkov radiation within the sphere. The scale length is set by the electron range in acrylic. The most energetic electrons from a ^{90}Sr source can emit Čerenkov radiation for a distance of about $R_c \simeq 9.3$ mm along their track length [8]. If total internal reflection is to be forbidden, then the radii must satisfy

$$r > n_{12}(R_c + r_i), \tag{1}$$

where n_{12} is the ratio of the refractive index of acrylic to that of the surrounding medium [9, 10]. The inner radius was set at $r_i \simeq 6.35$ mm in order to accommodate enough radioactive solution in the cavity. The outer radius was chosen to be $r \simeq 25.13$ mm, so that relation (1) is satisfied for any external medium.

The sources were made according to the following prescription: A known activity of ^{90}Sr solution is injected into the sphere in the form of a weak (0.1M) hydrochloric acid solution. The liquid is allowed to evaporate, leaving the ^{90}Sr behind, and the sphere is then sealed. The amount of activity present is estimated by weighing the source before and after injection of the solution.

The concentration of the ^{90}Sr solution (458 kBq per gram of solution) is quoted by the supplier, Amersham International plc, to an accuracy of $\pm 1.2\%$ (sys) $\pm 0.3\%$ (random). This measurement is made using a liquid scintillation counter with 4π efficiency, and the measurement technique is accredited by the National Measurement Accreditation Service. The only other radionuclide present in the solution at a significant level (apart from the yttrium daughter) is ^{137}Cs, which represents 14 ppm of the total activity. Since acrylic is manufactured from a distilled monomer, it is assumed that it does not contain significant activity. We will further assume that no activity is lost in the evaporation process.

In some prototype sources, there was a slight trace of powder left behind after evaporation of the hydrochloric acid. This is all the non volatile dissolved material, including the ^{90}Sr. This covers such a small area of the inner (spherical) surface, that it was thought to be negligible from a optical point of view. Indeed this powder is so thin that one can actually see through it. The grain size and diffuse nature of this powder mean that little energy is lost before an electron reaches the acrylic. Also, some electrons pass through the air inside the inner sphere. Typically an electron loses several keV in materials other than acrylic, and this introduces an error of about 0.5 % in our estimate of the Čerenkov light output. The sources are sealed using a thin brass screw. By defining a conductive path from the outside of the sphere, this also eliminates electrostatic charging of the beta source. This is because the surface conductance of acrylic is much greater than the bulk conductance, and so a conductive equipotential is established to the outside of the sphere.

3 Acrylic properties

We have used an acrylic similar to the type to be used in the SNO vessel. It is manufactured by the Polycast Technology Corporation. We have used data from many sources to determine the relevent parameters, optical transmission, refractive index and density. The density of acrylic is known to be about $\rho = 1.18$ g/cm^3. The density of the acrylic used was checked and was found to be $\rho = 1.182 \pm 0.004$ g/cm^3 at ambient temperature. The reproducibility of such measurements is limited, as acrylic is known to absorb water (vapour in the air) which increases

its density. The value assumed henceforth is $\rho = 1.182$ g/cm^3, with a (conservative) error estimate of 0.5 %. Since the amount of total Čerenkov radiation produced from a stopping electron is inversely proportional to the density of the medium, for a known stopping power, this will translate into a systematic error of 0.5 % in the light output.

The refractive index of acrylic is a slowly varying function of frequency, with values typically $n \sim 1.5$ for wavelengths about 400 nm. The production of Čerenkov radiation is quite strongly dependent on the refractive index, so an assumption of a constant refractive index will lead to systematic yield errors at the few percent level. This can be seen quantitatively from the theory of Frank and Tamm [11], see Jelley [6], which predicts the yield of N Čerenkov photons per unit angular frequency $d\omega$, per unit track length dx, from an electron of velocity βc, as

$$\frac{d^2N}{d\omega\, dx} = \frac{\alpha}{c}\left(1 - \frac{1}{\beta^2\varepsilon(\omega)}\right) \qquad \text{when} \qquad \beta^2\varepsilon(\omega) \geq 1\,, \tag{2}$$

where $\varepsilon(\omega) = n^2$ and α is the fine structure constant. Defining the electric susceptibility as $\chi_e(\omega) \equiv \varepsilon(\omega) - 1$, the yield $Y(\omega, \beta)$ becomes

$$Y(\omega,\beta) \equiv \frac{d^2N}{d\omega\, dx} = \frac{\alpha}{c}\left[\frac{\chi_e(\omega) + (1-\beta^{-2})}{\chi_e(\omega)+1}\right]. \tag{3}$$

For the ^{90}Sr sources many decays produce relativistic electrons with $\beta \to 1$ and for these cases the fractional error in the yield $Y(\omega, \beta)$ is about a third of the fractional error of χ_e.

Detailed measurements of the refractive index of acrylic have been made by Roehm Limited on a similar acrylic, covering wavelengths in the range 350 nm to 1000 nm. Their data are believed to be accurate to a few tenths of a percent, and we would like to use these data for our acrylic. However we cannot assume that the two acrylic samples are identical, and so the refractive index was measured for the acrylic sample used. The measurement was performed at ambient temperature with a sodium lamp to define the wavelength at 589 nm. The result was $n = 1.4956 \pm 0.008$, which gives an electric susceptibility of $\chi_e = 1.237 \pm 0.024$. This value is consistent (at the level of about 0.6 standard deviations) with the value from the Roehm measurement (made to standard DIN 53491) which is $\chi_e = 1.223 \pm 0.003$. We will henceforth adopt the Roehm values of the refractive index for our acrylic to the accuracy of the verification check. This will further enable us to reduce the systematic effects of the frequency dependence of the refractive index.

We note that the frequency dependence of the electric susceptibility $\chi_e(\omega)$ can be fitted quite well (in the optical region) to a damped Lorentzian shape, predicted by a simple model of atomic polarizability, due to a single atomic resonance [12]. The damping is quite weak, hence the long attenuation lengths found at visible wavelengths. The susceptibility of acrylic may have many such resonances, and the susceptibility $\chi_e(\omega)$ is a slowly varying function of ω, so the fit is probably not significant. In practice a smooth fit can be obtained with a Taylor expansion of $1/\chi_e(\omega)$ in powers of ω, and we have used a 7 $^{\text{th}}$ order fit to interpolate between the data. This fit, along with the Roehm data, is shown in figure 3. The fit is only assumed in the region between the first and last data points. Again the errors assumed in such cases are those from the accuracy of the verification check.

The optical transmission of the acrylic sample is crucial to the simulations of the amount of Čerenkov radiation leaving the sphere. The selected acrylic is believed to transmit in the ultra-violet. To verify these ultra-violet transmission properties, a sample of the acrylic was measured with a Perkin-Elmer Lambda-9 spectrophotometer. The sample had two parallel faces separated by 51.0 mm. The basic measurement procedures are those used by Davidson *et al* [13].

The bulk transmission of the acrylic is important to studies of the propagation of photons out of the sphere. For a medium with a refractive index described by the optical parameters $n(\omega)$ and $\kappa(\omega)$, the bulk transmission is given by:

$$T(\omega) = \exp\left(\frac{-4\pi\kappa x}{\lambda}\right) . \tag{4}$$

The interface (air/acrylic) reflection is then given by

$$R(\omega) = \frac{(n-1)^2+\kappa^2}{(n+1)^2+\kappa^2} . \tag{5}$$

In the optical wavelength region, the values of κ are typically $< 10^{-6}$, which enables us to neglect the κ^2 terms in equation (5). The raw transmission data are first corrected for the interface transmission losses. This is done to a sufficient accuracy by simply approximating a transmission $1 - R(\omega)$ across each interface. The values of $R(\omega)$ at each ω are calculated from the Roehm refractive index data. The scale distance travelled by a photon before leaving the sphere is about 15 mm, and the data are then scaled using equation (4) to give the bulk transmission over a distance of 15 mm. These data are shown in figure 4.

To interpret these data properly one must allow for the effect of scattering of the beam from diffuse reflections, surface scratches, Rayleigh scattering and impurities. These effects all mimic bulk attenuation in measurements of this type. The data in figure 4 show clearly that the acrylic transmits well above about 350 nm, and that the data are consistent with those from Davidson *et al.* The bulk attenuation cannot be accurately deduced from our data due to the scattering effects from the uncertain surface quality. It is generally possible to put a lower limit on the attenuation length, but difficult to establish an upper limit. The studies of Davidson *et al* show that above about 370 nm this particular acrylic has an attenuation length greater than 1 m. As Davidson *et al* report, the careful work of Christ and Marchic [14] suggests that the attenuation length in acrylic may be significantly greater than this.

The acrylic spheres have the simplifying feature that they are (approximately) spherically symmetric and the emitted Čerenkov radiation is assumed to be isotropic. Only bulk attenuation can reduce the light output; (non-attenuating) scattering processes have no effect on an isotropic source. The calculation of the amount of Čerenkov radiation which leaves the acrylic sphere is complicated by the possibility that the acrylic has a non-negligible bulk attenuation. The measurements of the acrylic bulk attenuation are all consistent with an arbitrarily large attenuation length. We have insufficient evidence to correct for optical attenuation, but the possibility of significant attenuation entails some uncertainties. If we take the lowest of the reported lower limits on the attenuation length, we have a systematic error at the 2 % level for the probability of Čerenkov photons leaving the sphere into a vacuum. For a sphere in water this uncertainty is slightly reduced due to the greatly improved transmittance of the acrylic/water interface which results in fewer photons being reflected back into the sphere. This systematic error is thus reduced to about 1.5 % in this case.

4 Calculations of total Čerenkov yields

Our aim is to calculate the number of Čerenkov photons per unit frequency produced from an electron of initial kinetic energy E_i stopping in an acrylic medium of relative permittivity $\varepsilon(\omega)$. We have performed two (nearly independent) calculations of this number which use a direct integral evaluation and a simple Monte-Carlo procedure. Both of these methods assume the theory of Frank and Tamm. We do not calculate the directional nature of the

photons as our sources are assumed to be isotropic when averaged over many events. The contribution from the (external) Bremsstrahlung photon spectrum is negligible in comparison to the Čerenkov radiation at optical wavelengths, see Jelley [6], section 3.10. Experiments with high energy pions and protons have shown that acrylic is a very poor scintillator, and for particles above the Čerenkov threshold, scintillation light is negligible compared to that from Čerenkov radiation.

For low energy electrons ($\gamma < 5$) we may approximate the shower as a single electron which loses energy continuously through the medium at a rate given by the tabulated stopping powers [8]. To calculate directly the total yields of Čerenkov radiation we need to integrate equation (3) along the electron track. The kinematic relationship between displacement and energy is then provided by the stopping powers. The integral is thus transformed to an energy dependent one, having the upper limit of the initial kinetic energy E_i and a lower limit of the Čerenkov threshold $E_t(\omega)$. The number of Čerenkov photons dN produced per unit angular frequency $d\omega$ is then

$$\frac{dN}{d\omega}(\omega) = \int_{E_t(\omega)}^{E_i} Y(\omega,\beta) \left(\frac{dE'}{dx}\right)^{-1} dE' , \qquad (6)$$

where dE'/dx is the electron stopping power of the medium and $Y(\omega,\beta)$ the yield function defined in equation (3). Since $Y(\omega,\beta)$ is a function of the velocity βc, the yield function can also be expressed as a function of the kinetic energy E'.

A simple simulation of a stopping electron has been implemented using the EGS4 code system [15]. This code enables us to simulate the electron shower through the acrylic. We are able to include the Čerenkov radiation contributions from pair production and knock-on electrons (δ-rays). This method treats each electron interaction in a statistical manner rather than on an average (continuous) basis, and thus electron 'straggling' is weighted more accurately than in the integral method. The code also gives the contribution to the Čerenkov radiation from the initial electron only, for comparison with the direct integration method. The code was implemented with the fractional energy loss per step (ESTEPE) set at 1 %. All electrons were tracked until their kinetic energy fell below the parameter AE, which was set at 150 keV. This is below the threshold for production of Čerenkov radiation at about 175 keV. The EGS4 predictions for the total yield of Čerenkov radiation were found to be robust under changes of the internal parameters AE and ESTEPE. The errors from varying these parameters suggest that systematic variations due to parameterization amount to about 1 % from varying AE in a region below the Čerenkov threshold and a fraction of a percent from varying ESTEPE.

The results of the two calculations are shown in figure 5. The data show the predicted total yields of Čerenkov radiation for electrons of initial kinetic energy E_i stopping in a medium of refractive index 1.5 (which corresponds to a wavelength of about 550 nm in the acrylic used) and density 1.182 g/cm^3. The data from the two calculations are in good agreement (0.5 %) for energies less than a few MeV. Near the Čerenkov threshold there is a systematic disagreement between these calculations, but since the contribution to the total yield is so small at this point, this disagreement is negligible. Above several MeV, the direct integration method predicts significantly less light than the EGS4 Monte Carlo. This is due to the contributions from δ-rays and pair production, which are included in the EGS4 calculation, but omitted from the direct integration technique. When the EGS4 simulation is modified to estimate the light from the initial electron only, good agreement is restored.

This agreement shows there are no significant calculational flaws in the prediction of the Čerenkov radiation. However both these calculations rely on accurate knowledge of the electron stopping power of the acrylic. The independence of stopping power data used in these

calculations is in some doubt, as both EGS4 and the ICRU table of stopping powers may contain some common physical assumptions which may not accurately reflect the behaviour of a stopping electron. Agreement at the 0.5 % level in the energy region of interest is a statement of the calculational uncertainty only.

Little experimental data is available to compare with the ICRU predictions. Paul and Reich [16] have measured the stopping power of several low Z materials at electron energies of 2.8 MeV and 4.7 MeV. Comparing the experimental data of Paul and Reich to the stopping powers predicted by the ICRU tables at 2.8 MeV shows that the predictions are systematically higher than the experimental values at the 97 % confidence level. The experimental values are systematically smaller then the ICRU tables by about 3 %. We do not have enough justification to correct the stopping powers for this difference as this correction will (presumably) be energy dependent. We have therefore included this 3 % as an estimate of the uncertainty of the stopping power of acrylic.

5 Beta decay

In order to determine the expected yield of Čerenkov radiation from beta decays within the acrylic spheres we integrate over the initial electron energy spectrum from the beta decays. From data given in the Tables of isotopes [17] and Nuclear Data sheets [18], we can summarize the decays :

1. The Strontium beta-decays to Yttrium with a half-life of 28.6 ± 0.3 years and an end-point energy of 0.546 MeV.

$$^{90}\mathrm{Sr}(\mathrm{J^P} = 0^+) \longrightarrow {}^{90}\mathrm{Y}(\mathrm{J^P} = 2^-) + e^- + \bar{\nu}_e \,. \tag{7}$$

2. The Yttrium beta-decays to Zirconium with a half-life of 64.07 ± 0.16 hours and an end-point energy of 2.2796 ± 0.003 MeV .

$$^{90}\mathrm{Y}(\mathrm{J^P} = 2^-) \longrightarrow {}^{90}\mathrm{Zr}(\mathrm{J^P} = 0^+) + e^- + \bar{\nu}_e \,. \tag{8}$$

The errors are deduced from the spread of reported values of these quantities. These decays are essentially free from gamma ray transitions. The largest of these is caused by a $\sim 0.01\%$ branch of the beta decay of ^{90}Y to a 0^+ level in ^{90}Zr, 1761 keV above the ground state. The nucleus then decays via an E0 radiative transition to the ground state with a half life of ~ 62 ps.

Both decays have $\Delta \mathrm{J} = 2\hbar$ and a parity change in the nuclear wave functions. Thus both decays are unique first forbidden transitions. If we define the (initial) electron kinetic energy E_i and $\gamma(E_i) = 1 + E_i/m_e c^2$, the relative probability density function $P(\gamma)$ of a decay becomes

$$P(\gamma) \sim \gamma F(Z,\gamma)(\gamma^2-1)^{1/2}(\gamma_0-\gamma)^2[(\gamma^2-1)+(\gamma_0-\gamma)^2]\,, \tag{9}$$

where $F(Z,\gamma)$ is the Fermi function and γ_0 is the value of γ at the endpoint. See Schopper [19]. We have ignored the effects of Rose screening on the beta decay spectrum. The relativistic Fermi function has the form

$$F(Z,\gamma) \sim (1+\delta)\,(\beta\gamma)^{2(\delta-1)}\, e^{\pi\nu}\, \frac{|\Gamma(\delta+i\nu)|^2}{|\Gamma(1+2\delta)|^2}\,, \tag{10}$$

where $\delta^2 = 1 - \alpha^2 Z^2$ and $\nu = Z\alpha/\beta$ where the electron velocity is βc. This probability spectrum is valid for both the Sr and Y decays with the appropriate end points and atomic

number Z. It is used to calculate the total Čerenkov yield from a single beta decay of both nuclei.

This is done by fitting a functional form to the integral yield data show in figure 5, by using a high order Taylor expansion about an arbitrary origin. The fit is made separately for the ^{90}Y and ^{90}Sr decays. The fit is observed to be very good for a wide range of choices of origin and fit order, and reproduces the yields to an accuracy of (at least) that of each data point (0.1 % random). Thus the calculation error is dominated by the systematic errors of the yield data calculated previously. The integral over the above probability spectrum is then performed using the above yield fit, and a numerical integration algorithm based on Patterson's method.

The small contribution to the photon spectrum from internal Bremsstrahlung has been estimated, but this is a negligible in comparison to the yield of Čerenkov radiation, and no correction is made.

6 Results and conclusions

We have computed the spectral intensity produced by the decay of a parent/daughter pair of ^{90}Sr/^{90}Y decays. The ^{90}Sr decay only contributes about 3 % of the Čerenkov radiation . We have found it convenient to treat the variation in the refractive index as a small perturbation of the result for $n = 1.5$. We have used the yield data from the EGS4 calculation, but the fractional change in yield from a small change in refractive index can be estimated to sufficient accuracy used the classical code. These yields and their variation with refractive index are tabulated in table 1. The resulting spectrum is shown in figure 6, along with 1 standard deviation error contours. The range of angular frequencies shown covers the range of vacuum wavelengths in the region 942 $\rightarrow$ 377 nm. The errors are not symmetrical as a failure of some of the assumptions made cannot increase the light yield. The errors are tabulated in table 2, but the uncertainty is dominated by the stopping power data. An additional uncertainty from the source activity must be included when estimating the total error of the Čerenkov light source. The total uncertainty is about 4%.

We have not attempted to estimate yields of Čerenkov radiation for wavelengths less than about 370 nm, because of the problems of bulk attenuation. In principle, this effect is calculable with an EGS4 and ray-tracing Monte Carlo. However, these calculations are quite sensitive to small changes in the bulk attenuation length, and since the Čerenkov yield increases at short wavelengths, these uncertainties are magnified to an unacceptable level. Consequently, our calculations predict the Čerenkov radiation for wavelengths greater than about 370 nm. In practise, light of shorter wavelengths is filtered out. In fact non ultra-violet grade acrylic may be ideal for this purpose, as it has a sharp short wavelength cut-off. A monochromator with known transmission could also be used. Some prototype sources were made with non ultra-violet acrylic to circumvent this problem, but external filtration gives greater flexibility.

The sources we have made contain several hundreds of kBq which gives intensities of the order of 10^{-8} Hz per unit angular frequency. There may be a requirement for sources of higher intensity, with perhaps 100 times the activity currently used. The amount of residual material deposited during the evaporation stage could be a problem here. We have considered dissolving this in acrylic monomer, and allowing the solution to polymerize in the source. There may be a requirement for calibrated sources with shorter wavelengths, perhaps as low as 300 nm. Acrylic may be unsuitable for such sources: we have considered fused Silica and glass as alternative materials.

Acknowledgements

R.J.B. would like to acknowledge the financial support of Thorn-EMI Electron Tubes Limited.

References

[1] G. Aardsma *et. al.*, (1987) *Phys. Lett.* B **194**, 321.

[2] R. S. Lakes and S. K. Poultney, (1971) *Applied Optics*, **10**, 4.

[3] A. T. Young and R. E. Schild, (1971) *Applied Optics*, **10**, 7.

[4] E. H. Belcher, (1953) *Proc. Roy. Soc.* A**216**, 90.

[5] W. Anderson and E. H. Belcher, (1954) *Brit. J. Appl. Phys.*, **5** (2), 53.

[6] Jelley, J. V. (1958) *Čerenkov radiation*, Pergamon Press, London.

[7] G. Present and D. B. Scarl, (1970) *Rev. Sci. Inst.*, **41**, 771.

[8] ICRU (1984). International Commission on Radiation Units and Measurements. *Stopping Powers for Electrons and Positrons*, ICRU Report 37 (International Commission on Radiation Units and Measurements, Bethesda, Md. 20814 USA).

[9] M. Born, and E. Wolf, (1965) *Principles of Optics*, Third (revised) edition, Pergamon Press, London.

[10] J. D. Jackson, (1975) *Classical Electrodynamics*, Second edition, Wiley, New York.

[11] I. M. Frank and Ig. Tamm, (1937) *Dokl. Akad. Nauk, SSSR*, **14** (3), 109.

[12] J. D. Jackson, *op. cit.*, section 7.5.

[13] J. C. Zwinkels, W. F. Davidson and C. X. Dodd, (1990) NRCC report 30789, to appear in *Applied Optics.*

[14] B. Christ and M. Marchic (1981) *Light scattering and absorption by glassy poly(methyl methacrylate) and polystyrene*, SPIE **297**, Emerging Optical Materials, page 169.

[15] Walter R. Nelson, Hideo Hirayama and David W.O. Rogers, (1985) *The EGS4 code system*, SLAC report 265.

[16] W. Paul and H. Reich, (1950) *Energieverlust schneller Elektronen in Be, C, H_2O, Fe und Pb*, Z. Phys. **127**, 429.

[17] E. Brown, J. M. Dariki and R. E. Doebler *et. al.*, (1978) *Tables of Isotopes*, Seventh edition, Wiley, New York.

[18] Nuclear Data Group, (1975) *Nuclear Data Sheets*, **16**, 1, Oak Ridge National Laboratory, P. O. Box X, Oak Ridge, Tennessee 37830, U.S.A.

[19] H. F. Schopper, (1966) *Weak Interactions and Nuclear Beta Decay*, North-Holland, Amsterdam.

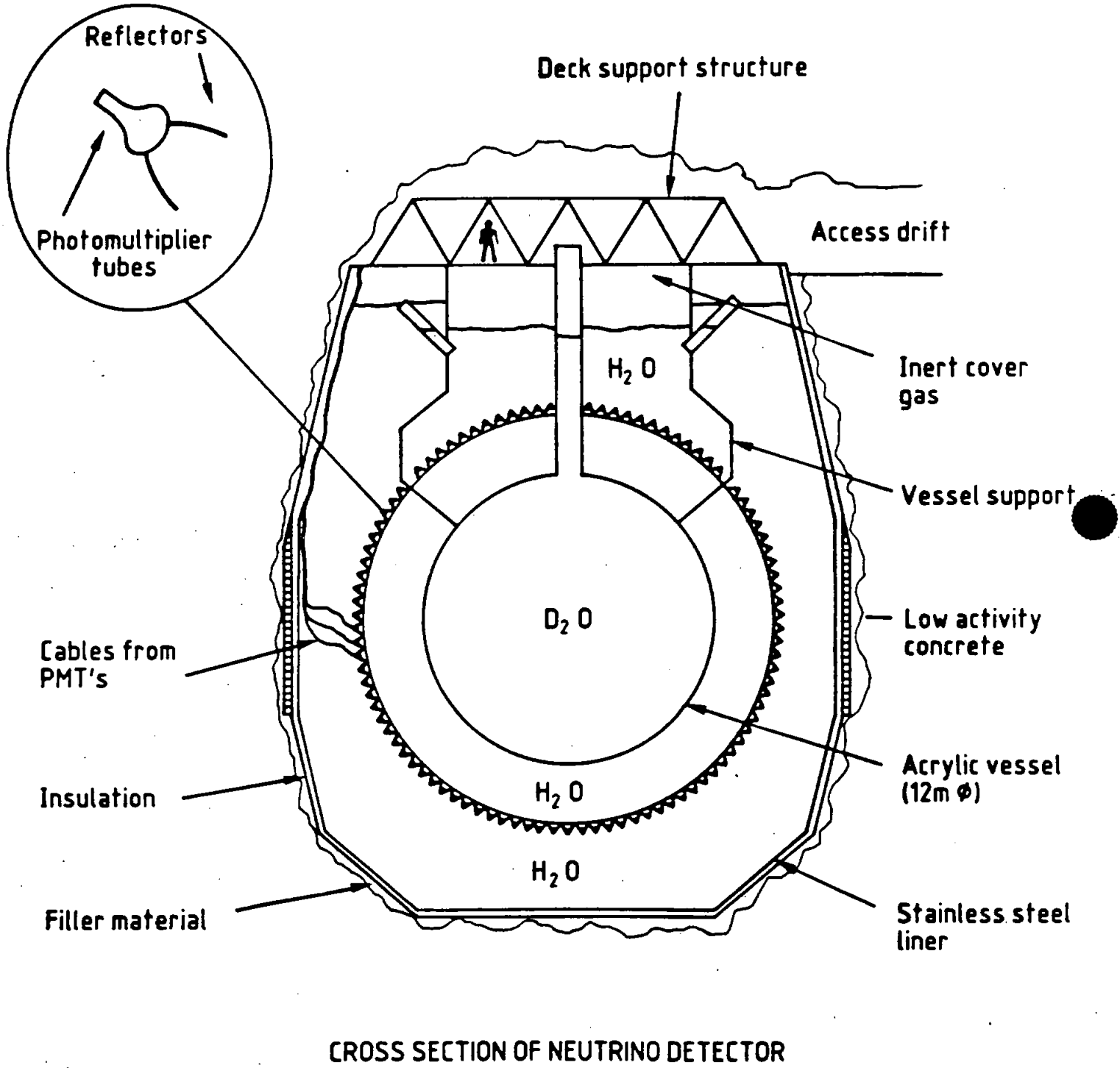

Figure 1. The SNO detector.

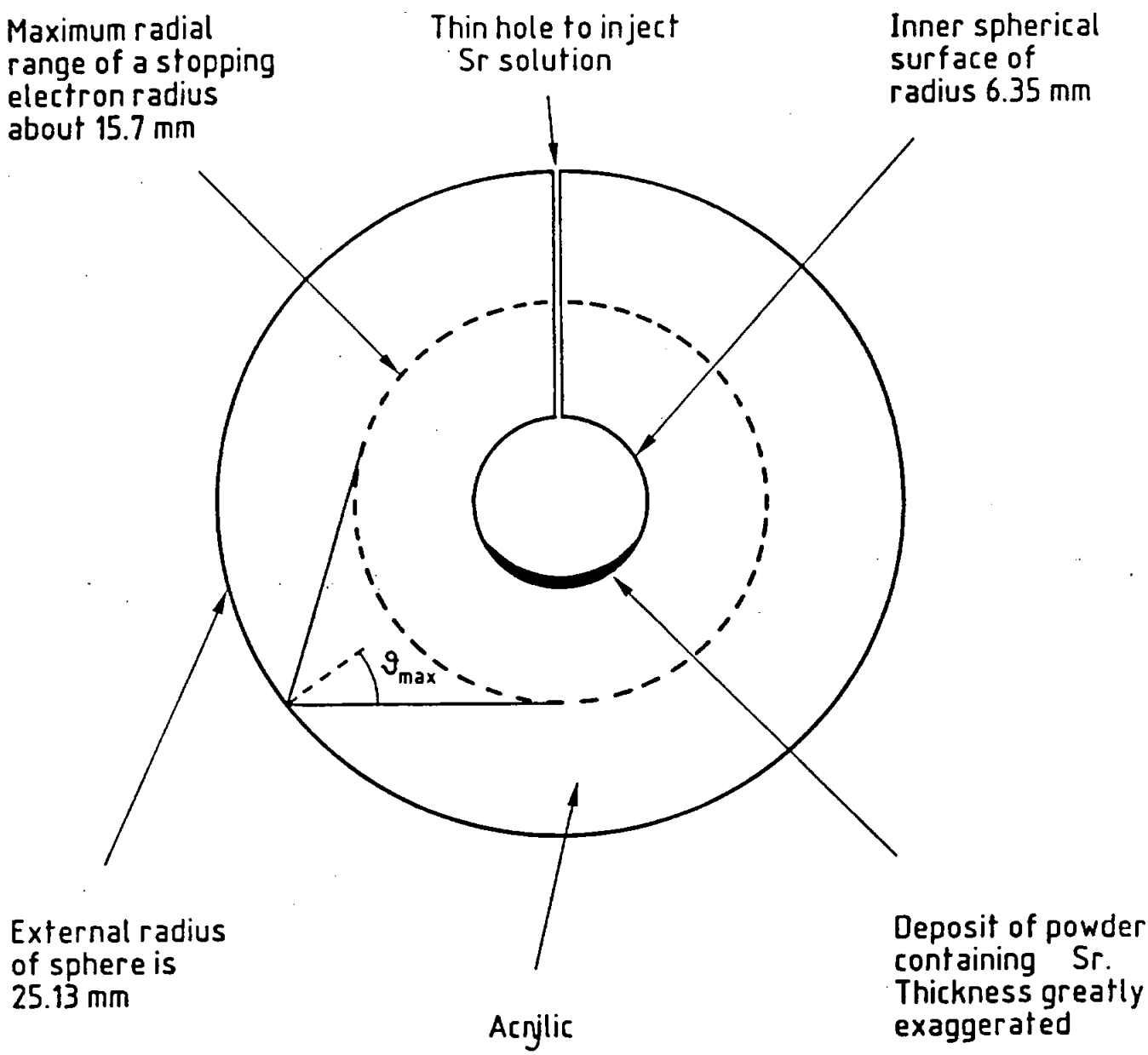

Figure 2. Cross-section of an acrylic sphere, showing the maximum angle θ_{max} with respect to the radial vector that a photon can have outside the sphere of maximum radial range. The sphere is designed so that no Čerenkov photons are totally internally reflected.

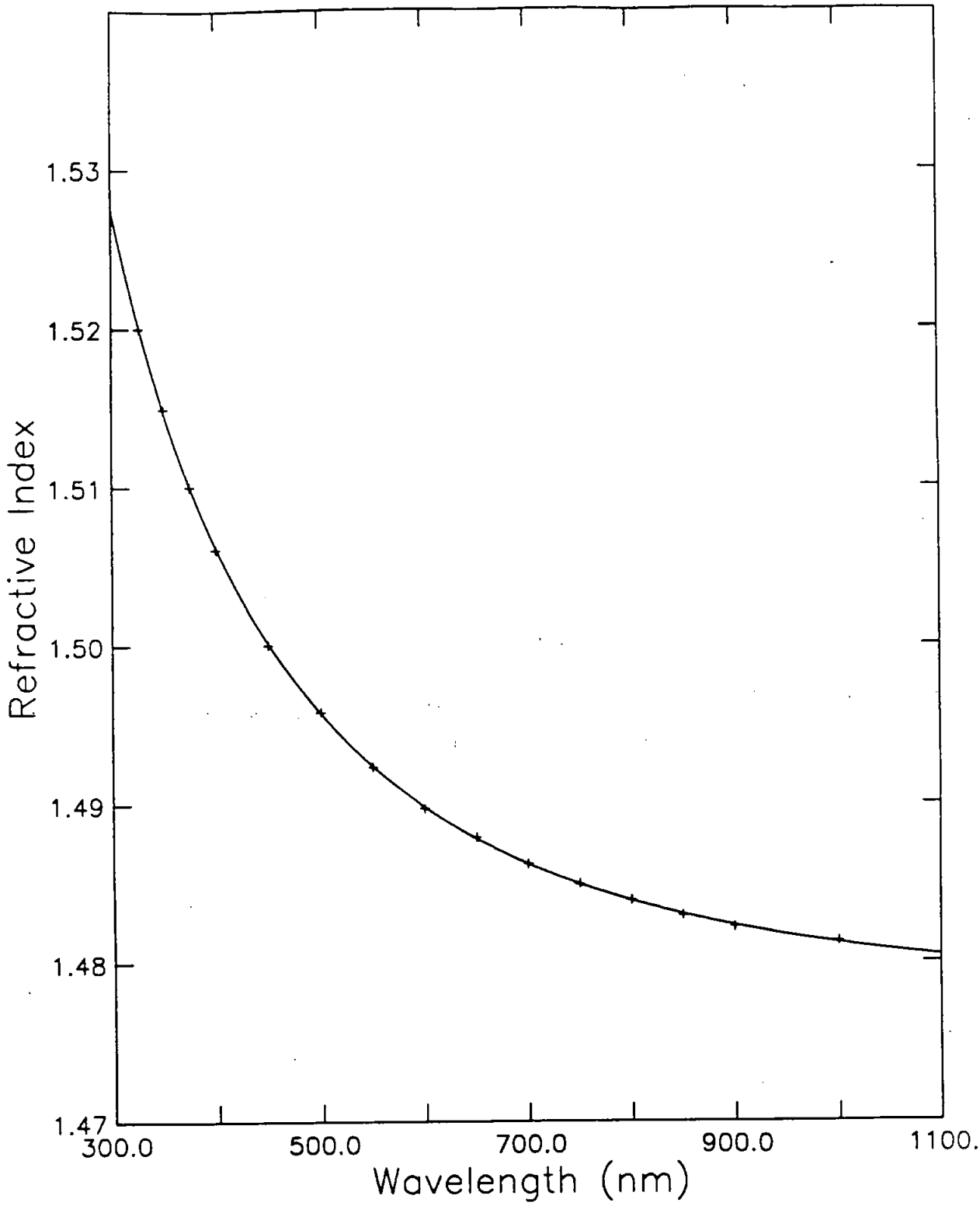

Figure 3. Acrylic refractive index. The + points show the Roehm data, and the solid curve is a 7^{th} order fit to these data.

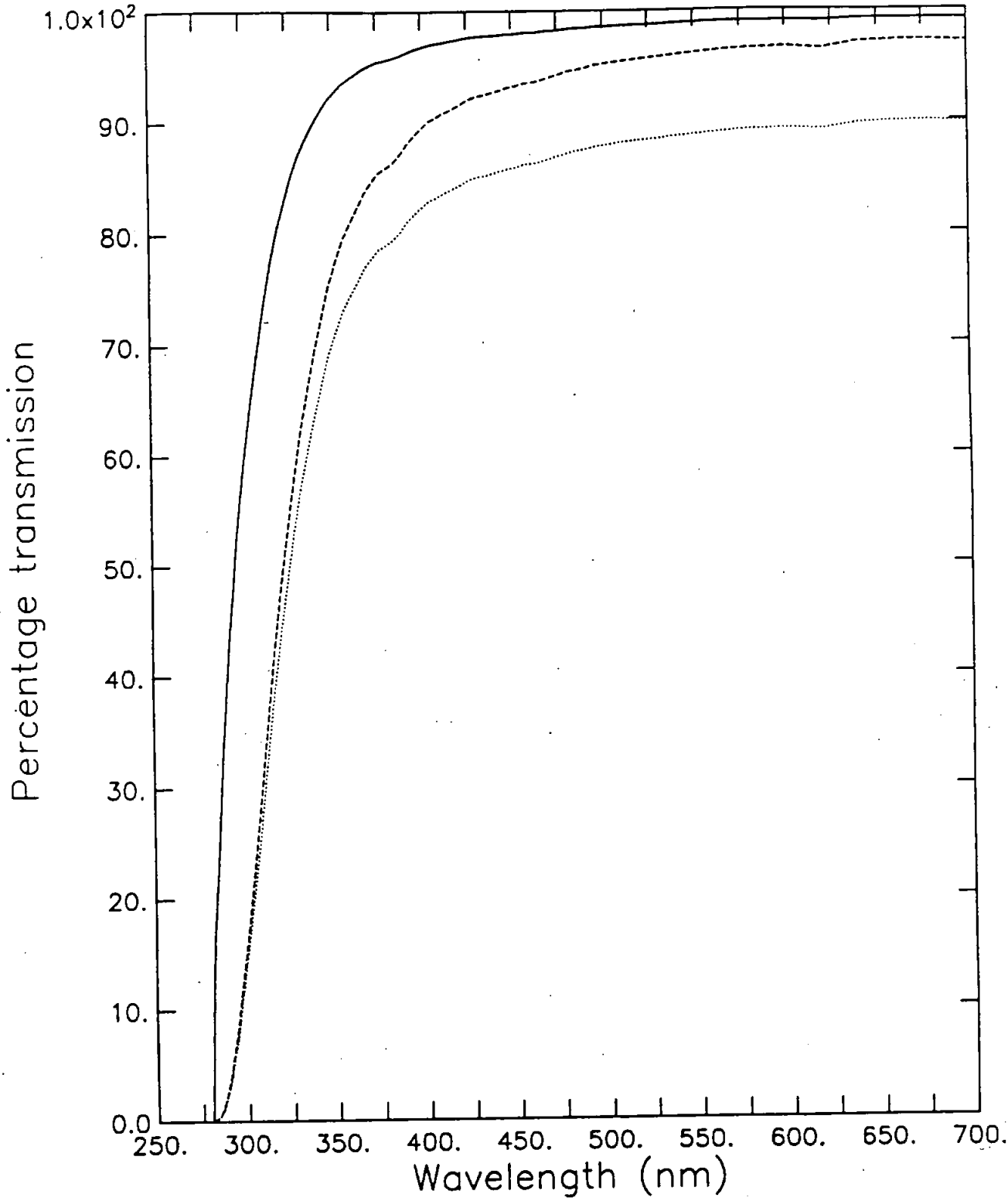

Figure 4. Optical transmission of Polycast acrylic. The dotted curve show the raw data from a 51 mm thickness, the dashed curve show the data without Fresnel reflections. This is then scaled to a thickness of 15 mm, shown by the solid curve.

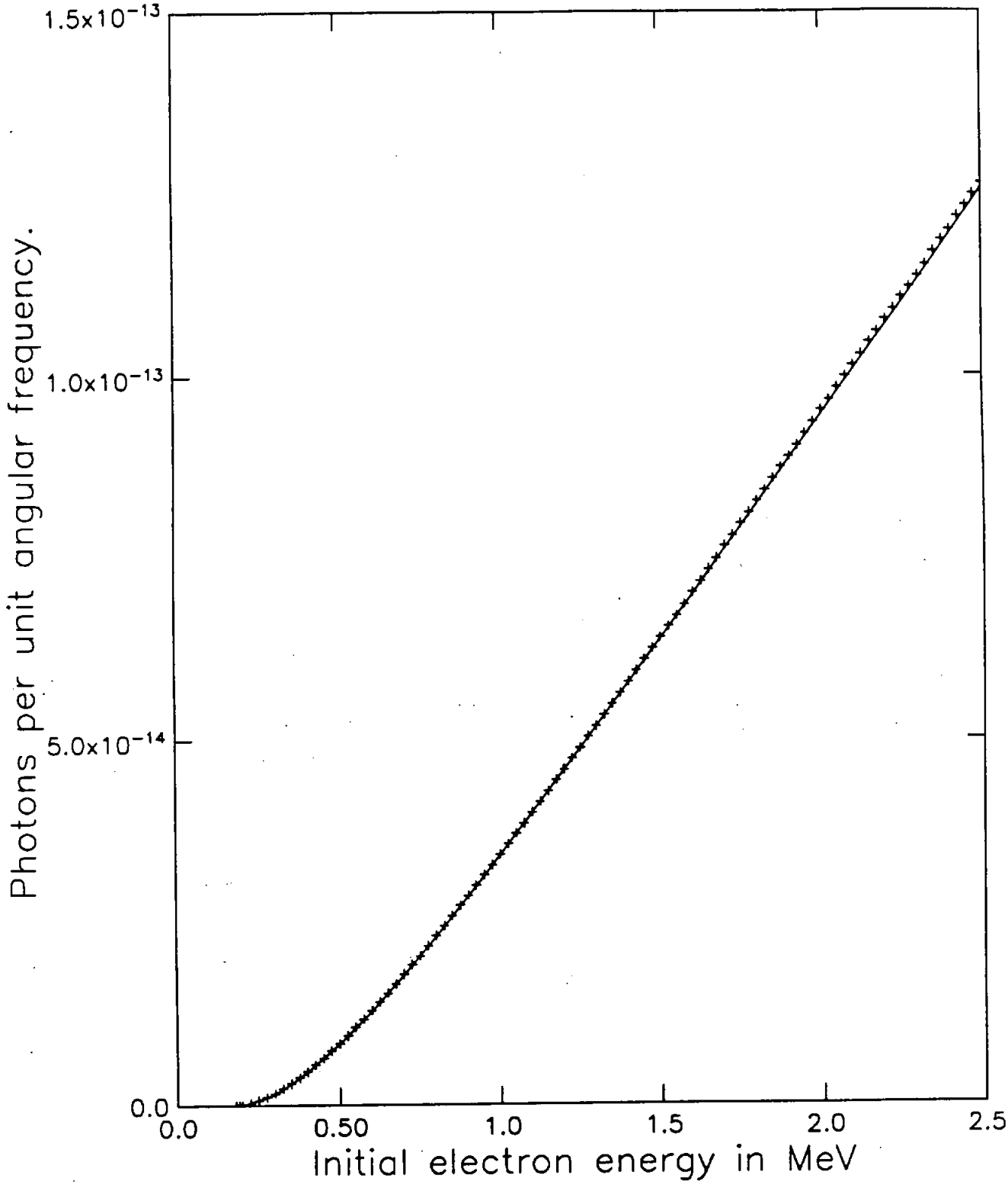

Figure 5a. The yield of Čerenkov photons ($dN/d\omega$) produced in acrylic. The Classical calculation (see text) is show by the solid curve, and the EGS4 predictions are shown by the + points. Both calculations assume $\rho = 1.182$ g/cm^3 and $n = 1.50$.

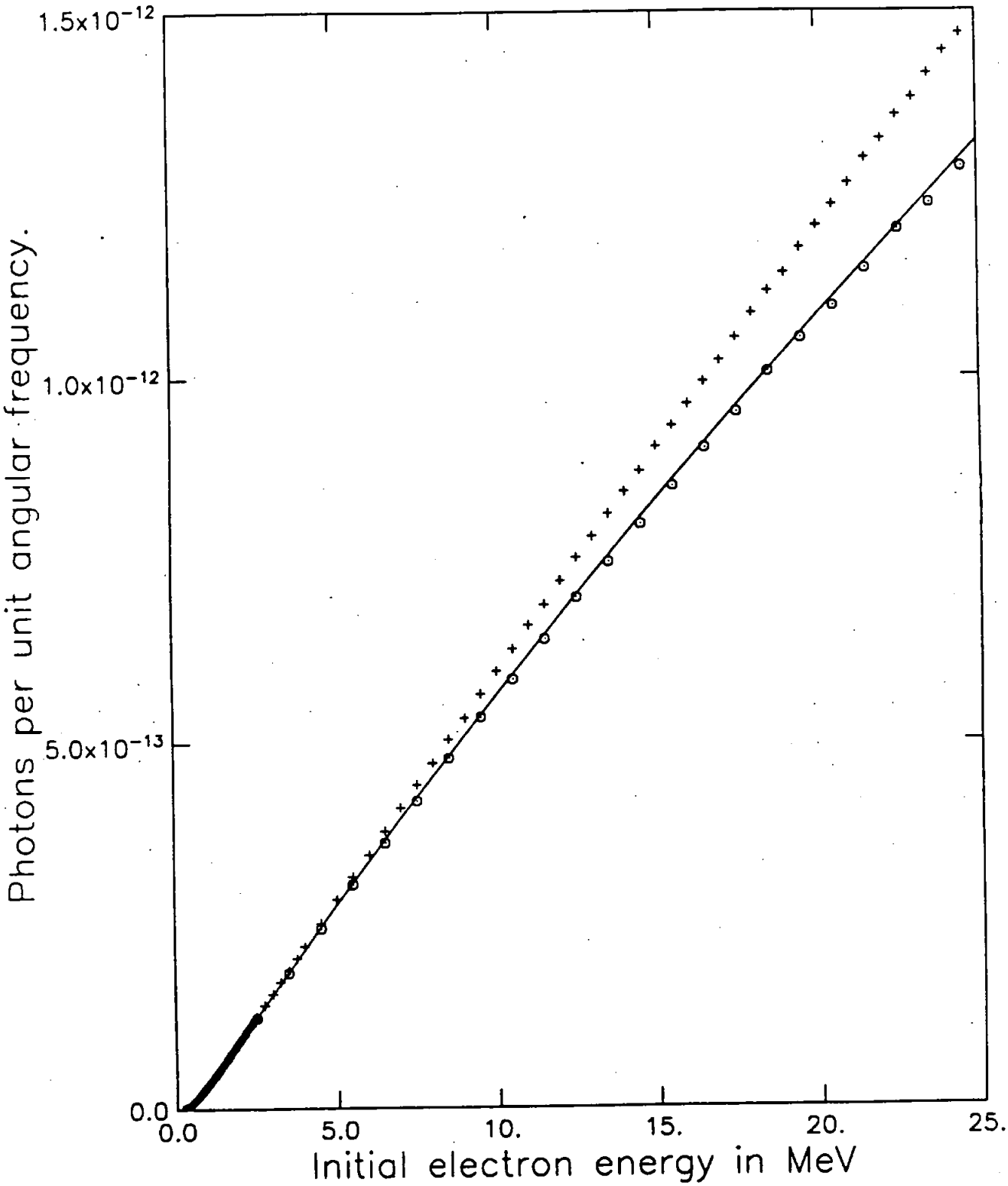

Figure 5b. Čerenkov yields for higher energy electrons. The circles show the predicted Čerenkov radiation yields from the initial electron only, using the EGS4 monte carlo. The + points and the solid curve are as figure 5a.

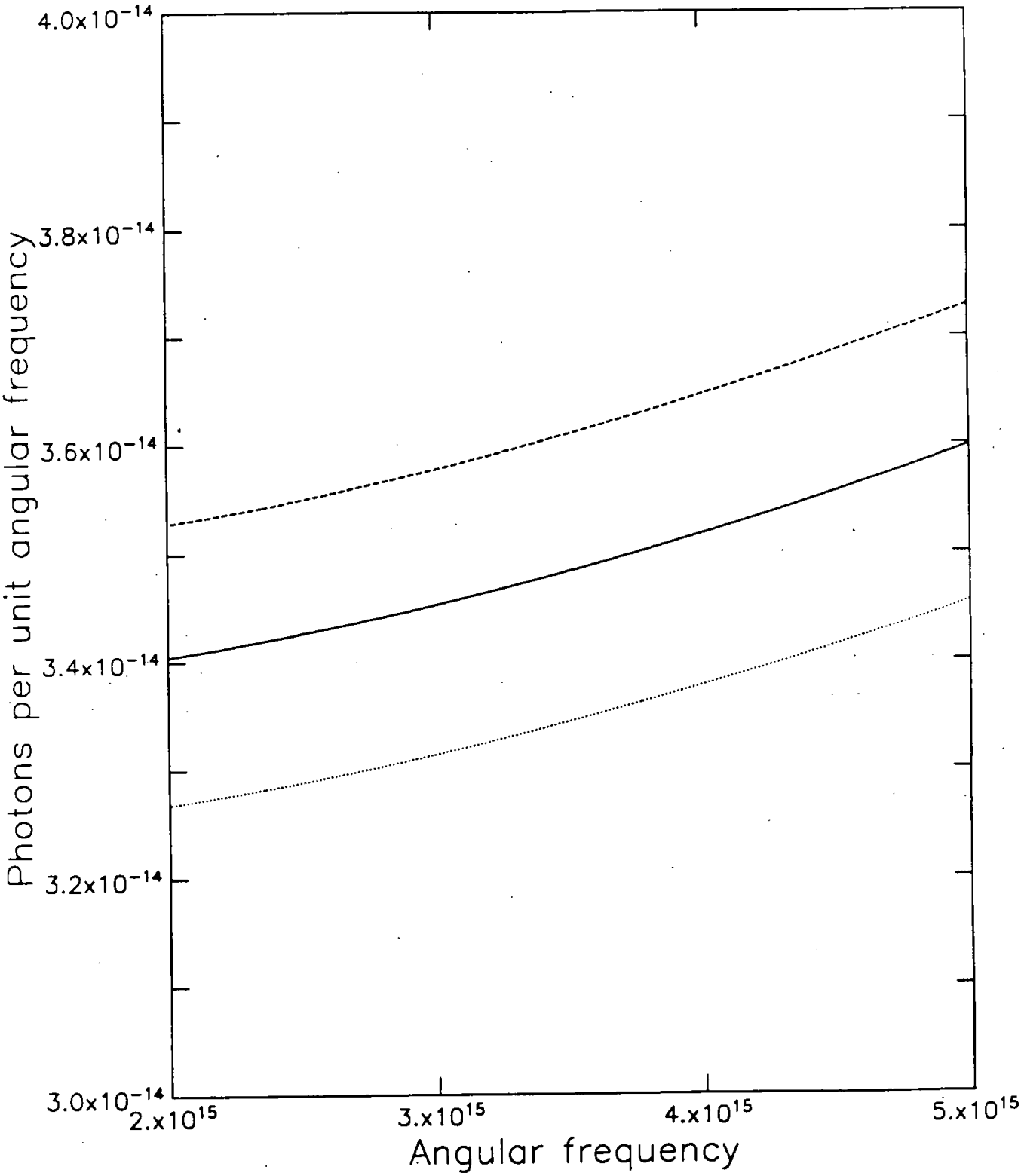

Figure 6. The total yield of Čerenkov radiation from the decay of a ^{90}Sr and ^{90}Y pair is shown by the continuous curve. The upper (dashed) curve shows the contour of a 1 standard deviation overestimate. The lower (dotted) curve shows the contour of a 1 standard deviation underestimate.